LAUR-075957

Space Surveillance One Photon at a Time

Jeffrey J. Bloch
Los Alamos National Laboratory
Richard Rast
Air Force Research Laboratory/DETE

ABSTRACT

Large format photon counting imaging sensors with high time resolution provide a unique capability for astrometry and object tracking from a moving or scanning observation platform. These sensors produce an output list of photon events in X, Y, and Time which can be transformed in a distortion-less manner to any fixed or co-moving coordinate system. In this presentation we discuss how this capability enables new approaches to space object detection and metric observation over traditional framing sensors such as CCDs using a specific, serendipitous set of observations as an example.

NASA's Galaxy Evolution Explorer (GALEX) ultraviolet astrophysics mission provides a unique opportunity to explore the utility of high time precision imaging photon counting sensors for space surveillance tasks. The 280 kg GALEX satellite was launched in 2003 by a Pegasus XL rocket into a 690 km circular orbit. GALEX contains a 50 cm NUV/FUV telescope with a field of view of 1.2 degrees and a 5 arc-second spatial point spread function. Each ultraviolet photon detected by GALEX is time stamped to a precision of 5 milliseconds and telemetered to the ground. In this paper we will discuss how to utilize GALEX X-Y-Time photon list data to detect and characterize space objects that serendipitously crossed its field of view. We show the results of how the high precision angle-angle-time GALEX photon data combined with the GALEX satellite's ephemeris can be used to detect a space object and derive a state vector for the object from a single field-of-view crossing. This can be done in ways very different from traditional framing sensors such as CCDs. Such analysis methods can be applied in general to any photon counting imaging detector system working at any wavelength on any ground, airborne, or space platform.

1. INTRODUCTION

Space surveillance applications require focal plane detectors with high sensitivity as well as good time resolution in order to perform angular metric observations for orbit determination. The detectors available for the focal planes of optical instruments including telescopes, cameras, and microscopes have evolved tremendously over history. Photographic glass plates gave way to plastic film emulsions of ever increasing quality. Early electronic imaging systems included Vidicons and hybrid film/electronic systems such as those on NASA's Lunar Orbiters. Optical information in the high time resolution domain was first provided by photomultiplier tubes, which had no intrinsic

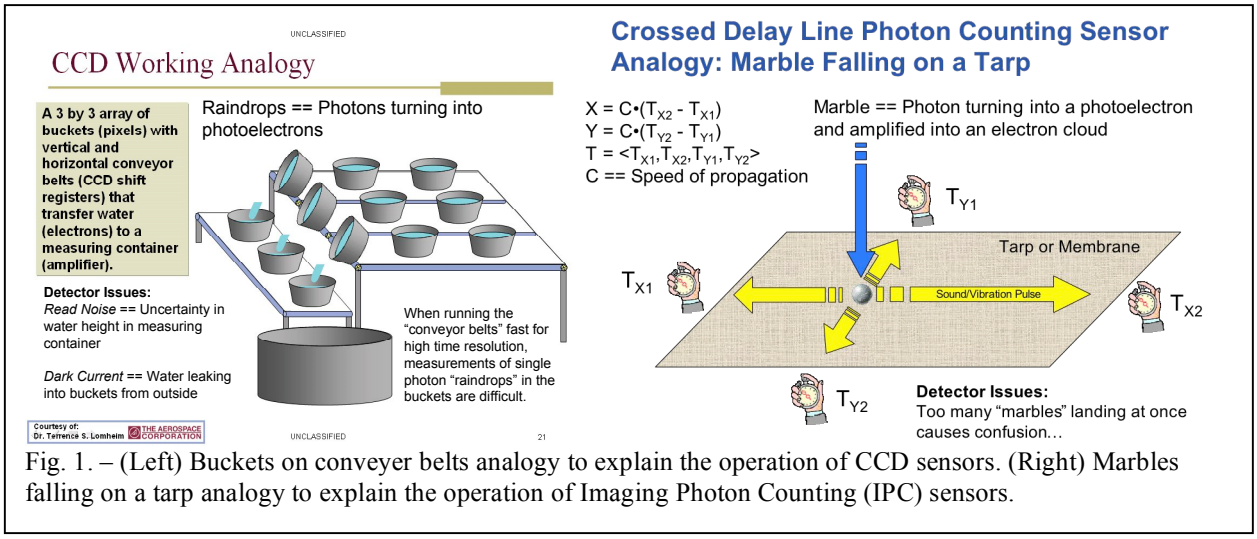

Fig. 1. – (Left) Buckets on conveyer belts analogy to explain the operation of CCD sensors. (Right) Marbles falling on a tarp analogy to explain the operation of Imaging Photon Counting (IPC) sensors.

spatial resolution. Charge coupled devices arrived on the scene with ever increasing format size, quantum efficiency, and reduced readout noise. CMOS sensor technology is rapidly catching up to CCD's capabilities and has the promise to reduce instrument complexity.

The perfect focal plane sensor would (to the quantum limit) record the time of arrival and spatial location on the focal plane as well as the wavelength and polarization for each photon. We do not have such detectors yet. The choices we currently have of detector technologies leaves us with tradeoffs in which we choose which of these quantities we can accurately and precisely measure simultaneously. Commercial pressures have accelerated the capabilities of pixilated silicon-based sensors (digital cameras with the format of older 35mm film cameras are available off the shelf). However, another class of sensor that works very differently is also available. High-performance microchannel plate Imaging Photon Counters (IPCs) [1] count, locate, and time tag photons that strike their surface, but are mostly available for specialized research applications and are less available commercially. In this paper we discuss these high-performance microchannel plate Imaging Photon Counters and their applicability for space surveillance using a specific serendipitous space borne example. We contrast the advantages of these sensors with traditional approaches involving CCD or CMOS sensors. We recognize that intermediate approaches such as Electron Multiplied Charge Coupled Devices (EMCCDs) and arrays of Avalanche Photodiodes (APDs) are beginning to fill in the technological no-man's land between these approaches but will not be considered here. APDs have yet to approach the spatial format required for the techniques discussed in this paper. EMCCDs do not yet have the time resolution and readout-noise equivalent to IPCs.

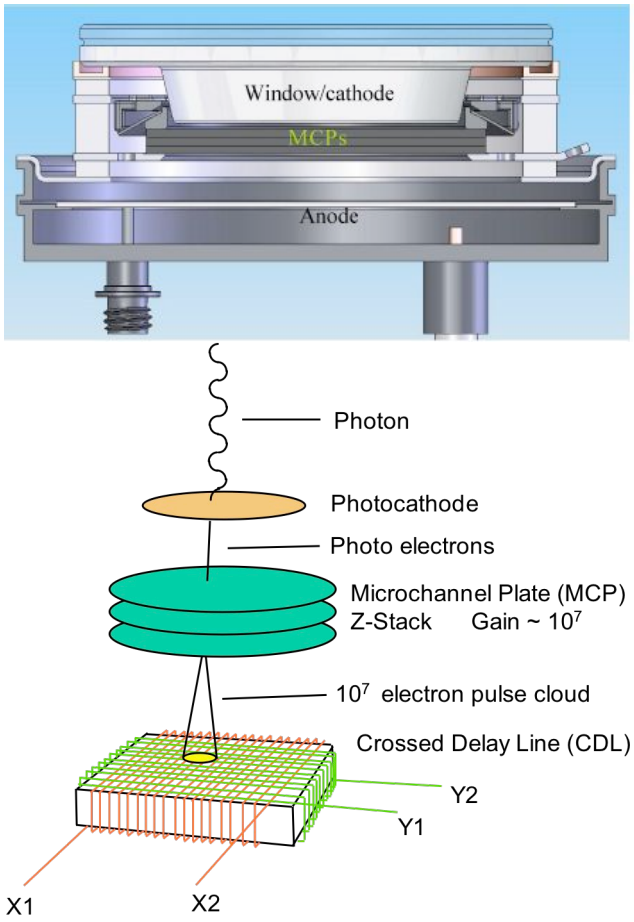

Fig. 2. – (Top) Internal layout of a typical high resolution microchannel plate imaging photon counter (IPC). (Bottom) Schematic operation of an IPC.

IPCs provide an output data list of each photon's spatial location and precise time of arrival on the focal plane. This paper explores how counting photons from the sky one at a time with IPCs can improve the capabilities for optical space surveillance.

2. PHOTON COUNTING VS. FRAMING SENSORS

Fig. 1 illustrates by analogy the qualitative difference between CCDs and IPCs. A CCD is an analog shift register, enabling analog signals (electric charges) to be transported through successive stages (capacitors) controlled by a clock signal. CCDs operate as if they were arrays of buckets fixed to conveyer belts. "Raindrops" falling in the buckets represent photo-electrons. These are created when photons enter the pixels on the silicon chip. The conveyer belts are stationary while an exposure takes place. Once the exposure is complete, the conveyer belts shift the collected water (first in one dimension and then the other orthogonal direction) to a "readout bucket". The readout bucket measures the water level (number of photo-electrons) contained in each of the conveyer belt buckets (pixels). To measure the arrival time of each "raindrop" or photo-electron with high precision, the conveyer belts have to run

faster. Soon the buckets are only collecting single photons or raindrops when operating under low light conditions. The measurement apparatus has difficulty when trying to measure "single raindrops" in each bucket, as the readout noise is at best +/- one raindrop (electron).

In contrast, IPCs operate as if they are tarps or membranes stretched across a frame onto which amplified photo-electron "marbles" fall onto (Fig. 1). When the marble strikes the membrane, vibrations or sound waves travel to the four sides of the frame. The location of the marble striking the tarp can be computed using the precise difference in the time of arrival of the sound or vibrations at the four frame edges, and by knowing the sound or vibration propagation velocity. Fig. 2 shows the cross section and operation of one type of IPC. The incoming photons are detected and converted to electrons by a photocathode on an entrance window, or by an opaque photocathode

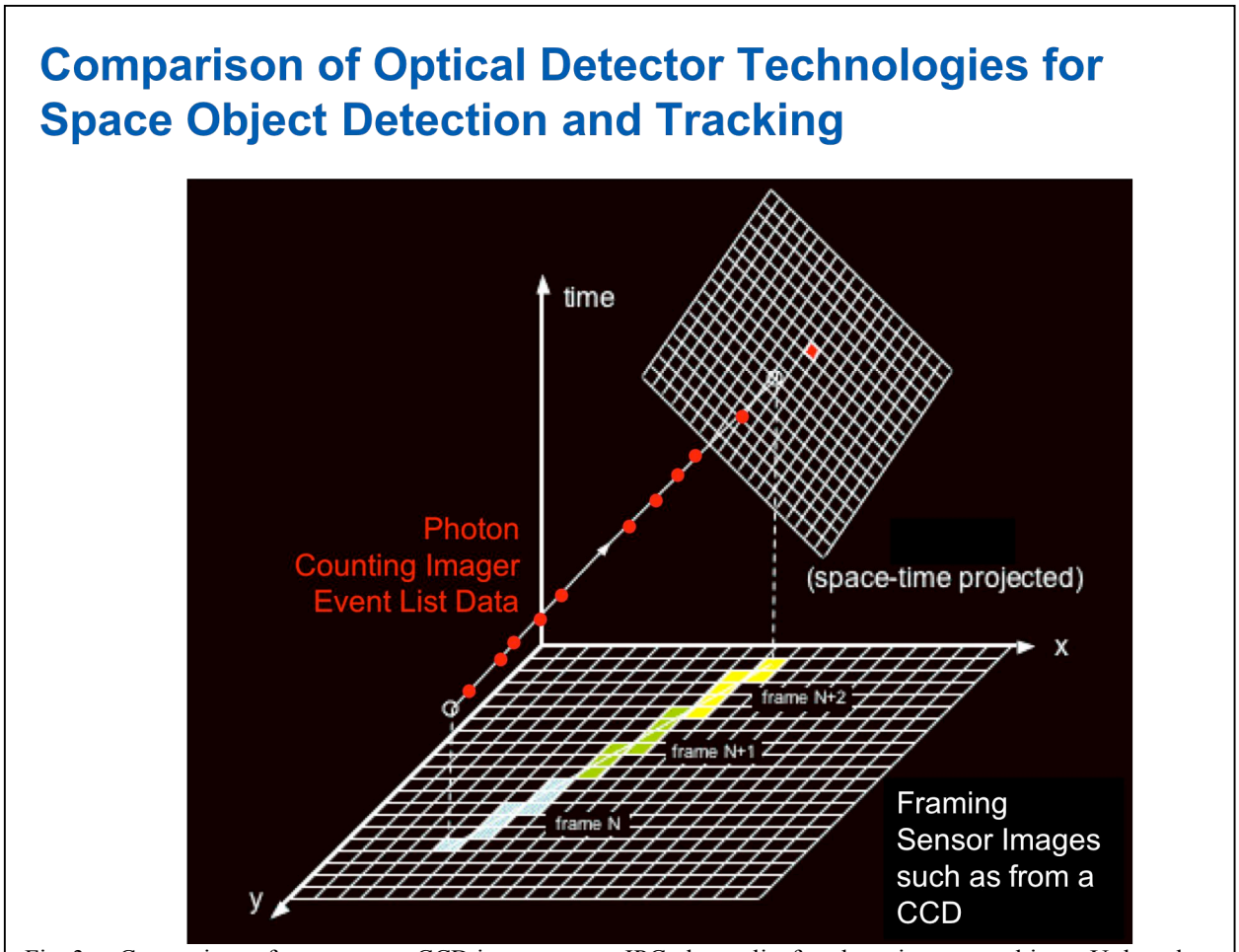

Fig. 3. – Comparison of one or more CCD images vs. an IPC photon list for detecting space objects. Unless the CCD sensor "rate tracks" the moving object (either electronically or with mechanical tracking) the photons from the object are smeared out and diluted across the focal plane and mixed in with diffuse background light and starlight. In contrast, time tagged photon list data can always be projected onto a plane in the Position-time 3D space (equivalent to a commoving coordinate system) in which all the photon events from the space object track fall into a single "virtual" pixel.

deposited onto the first microchannel plate (MCP) of a stack of MCPs. The MCP stack typically has a gain of 10^7, depositing the resulting charge onto a delay line readout anode. Typical delay line schemes encode photon event position centroids, by determination of the difference in arrival time of the event charge at the two ends of a distributed resistive-capacitive (RC) delay line. A workhorse delay line configuration is the cross delay line (XDL). In its simplest form the delay-line encoding electronics consists of a fast amplifier for each end of the delay line, followed by time-to-digital converters (TDC's). The ultimate resolution of delay line anodes in this scheme is determined by the event timing error. This is dominated by the constant fraction discriminator (CFD) jitter and

walk, and noise in the time-to-amplitude converter (TAC) part of the TDC, which is typically of the order ~ 10 ps FWHM total [1,2].

Priedhorsky and Bloch [4] discussed the enhanced capabilities of high time resolution IPCs for detection of moving space objects against the stellar background. Fig. 3 depicts the key idea differentiating IPCs from CCDs or other integrating framing sensors for space surveillance applications. The time tagged photon list from the IPC can be manipulated and projected onto a coordinate frame in which all the photons from a target object fall into a single detection cell. IPCs effectively enable "rate tracking in software" after the data are collected. This is superior to mechanical rate tracking or CCD techniques such as Time Delayed Integration (TDI) / Orthogonal Transfer Arrays (OTA) because the object's tracking rate does not need to be known during the observation. Movies can also be created from photon lists at arbitrary time resolutions to enhance the ability to detect moving objects. IPCs also enable searches for multiple objects with different and arbitrary velocities in the same data set.

3. GALEX SATELLITE

Our serendipitous opportunity to evaluate IPCs for space-based optical space surveillance arrived with the NASA Galactic Evolution Explorer (GALEX) satellite [1,3] (Fig. 4). The satellite was launched via an Orbital Sciences Corporation Pegasus-XL vehicle into a 29 degree inclination, 690 km circular orbit on April 28, 2003. After a two month in-orbit checkout period GALEX began nominal operations. At the heart of the instrument are two sealed tube photon counting detectors of 65mm active area. It has been successfully obtaining imaging photometric observations of astronomical sources in two ultraviolet bands (near ultraviolet [NUV] 1750 – 2750Å, far ultraviolet [FUV] 1350 – 1750Å). The

Fig. 4. – GALEX satellite.

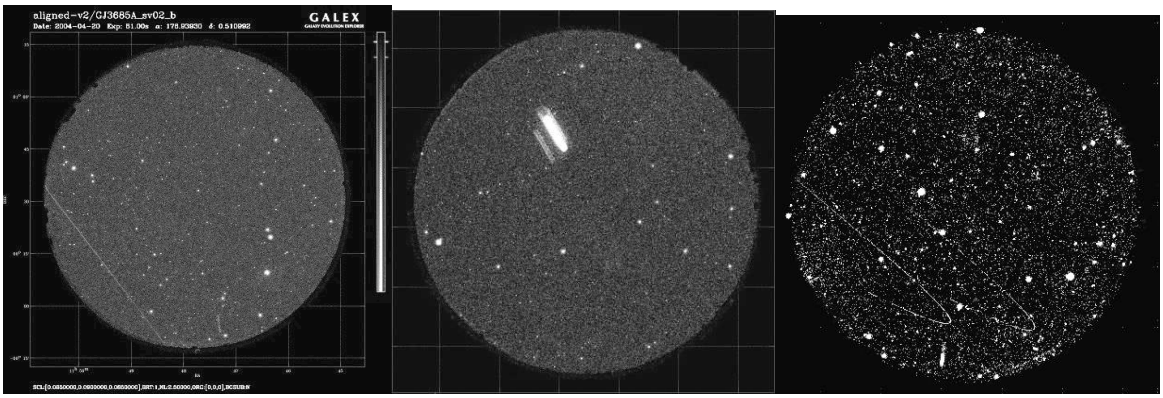

Fig. 5. – Depicted here are three examples of space objects serendipitously passing in front of GALEX's 1.2° field of view during an astronomical observation. From left to right, the amount of data displayed as an astronomical image is approximately 25 seconds, 19 seconds and 800 seconds respectively. The object in the middle image was so bright that small internal reflections in GALEX's optics are apparent. The objects in the right image demonstrate prograde-retrograde motion This is because they are geosynchronous objects viewed at nearly 90° to the Earth-GALEX line and so exhibit similar prograde-retrograde changes in apparent motion with respect to the stars as does Mars viewed from the Earth.

GALEX scientific instrument consists of a 50 cm aperture Ritchey-Chretien UV optimized telescope with a 1.2° field of view (~5 arc-second FWHM resolution imaging) and an optical wheel mechanism that allows the light-path to be selected for either two-band UV imaging or two-band UV spectroscopy through a dispersive grism. The scientific instrument is coupled to a three-axis stabilized spacecraft bus built by Orbital Sciences Corporation (OSC). The satellite attitude is dithered in a 1 arc-minute spiral for deep targets, while the all-sky survey is obtained by scanning at a rate of 200 arc-seconds/sec. Dithering and scanning is performed to average over detector non-uniformities and to prevent microchannel plate detector gain fatigue by UV bright stars. Despite the continuous scanning of the field-of-view, the photon data are assigned positions on the sky to within a 5.6 arc-second point

spread function. This is made possible by combining the photon's time of arrival and focal plane location with the satellite attitude data.

GALEX continuously collects data during orbit night and when outside of the South Atlantic Anomaly. These observation periods can last from 800 to 1800 seconds. Because GALEX continuously collects photon data during that time, there is a relatively high probability that a space object will serendipitously cross its 1.2° field of view. Fig. 5 depicts some examples of some bright object detections. This operation mode can be contrasted with another well-documented space based optical space surveillance sensor, the Space Based Visible (SBV) on the Midcourse Space eXperiment (MSX) satellite [5]. SBV is a CCD based system. SBV must re-orient and point its field-of-view between each 0.5 to 3 second exposure and subsequent readout and processing of the CCD data, and so has a much lower observation duty cycle. Table 1 compares the characteristics of SBV and GALEX.

Characteristic	**GALEX**	**SBV**
Field of View (Degrees)	1.2° Circular	1.4° x 6.6°
Wavelength Coverage (nm)	135-175/175-280	Visible
Limiting Detection Magnitude	20.5 (UV, 100s exp)**	12-15 (Vis)
Number of angular measurements per second per object	1-100's (each photon event is a "measurement")	0.5-2 (Streak end-points are the "measurements")
Pixel size or PSF (arc-seconds)	5.6"***	12"
Astrometric Accuracy (arc-sec)	0.5"	4"
Time Resolution (Seconds)	0.005	??

Table 1 – Characteristics of GALEX and SBV. ** Because the Sun is 5 magnitudes dimmer in the UV than in the visible, GALEX has a comparable or slightly better (dimmer) object detection threshold than SBV.***Photon events are digitized to locations much better than an arc-second on the GALEX focal plane, so the combined optical and electronic PSF is well over-sampled.

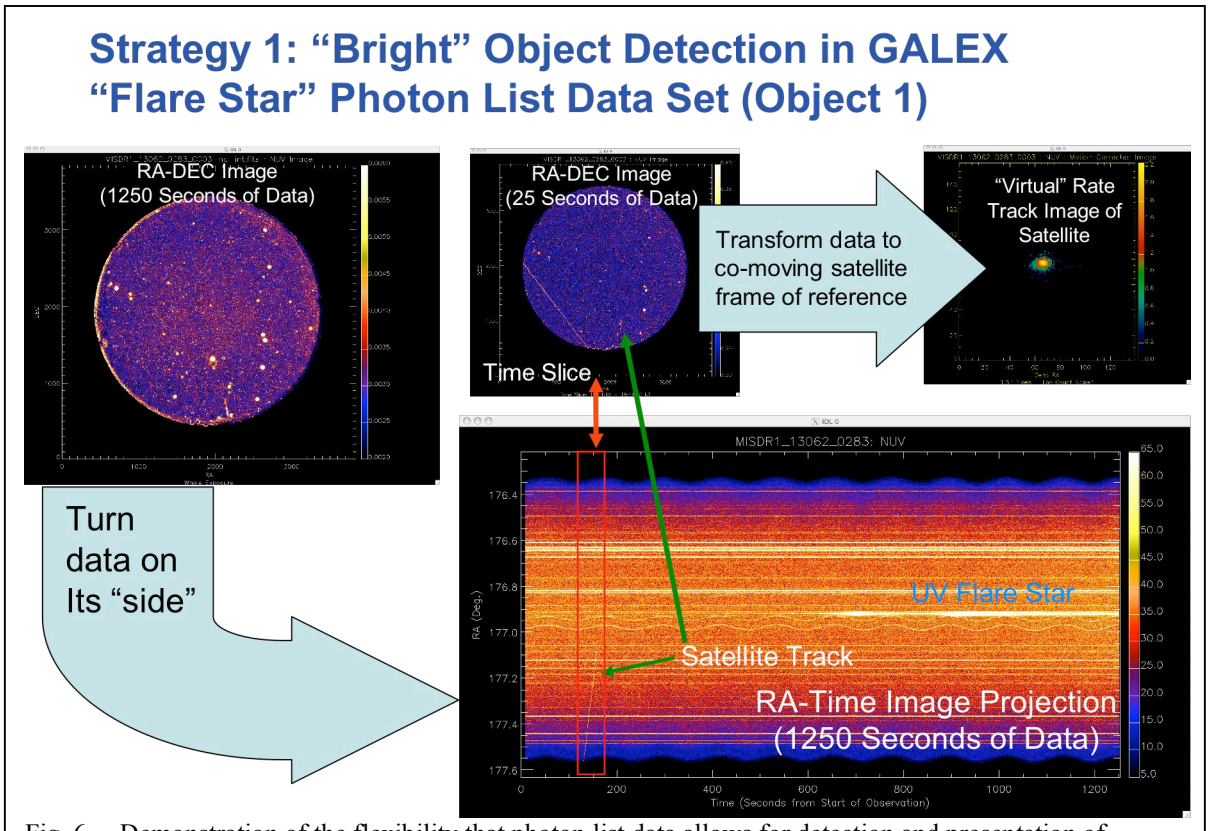

Fig. 6. – Demonstration of the flexibility that photon list data allows for detection and presentation of photon events from a moving object.

4. OBJECT DETECTION STRATEGIES AND EXAMPLES USING GALEX DATA

In this section we will examine one GALEX dataset (1250 seconds of continuous data collection) that contains at least two objects that transited GALEX's field of view. The first object is relatively bright and crossed a corner of the field of view for about 25 seconds. The object exhibited a count rate of ~160 photon events per second corresponding to an NUV magnitude of 14.5. These objects are illuminated by the NUV flux from the Sun which is 5 magnitudes dimmer than in the visible portion of the spectrum. All other things being equal (e.g. the albedo of the object), this first object would probably be a magnitude 8 or 9 object in the visible portion of the spectrum.

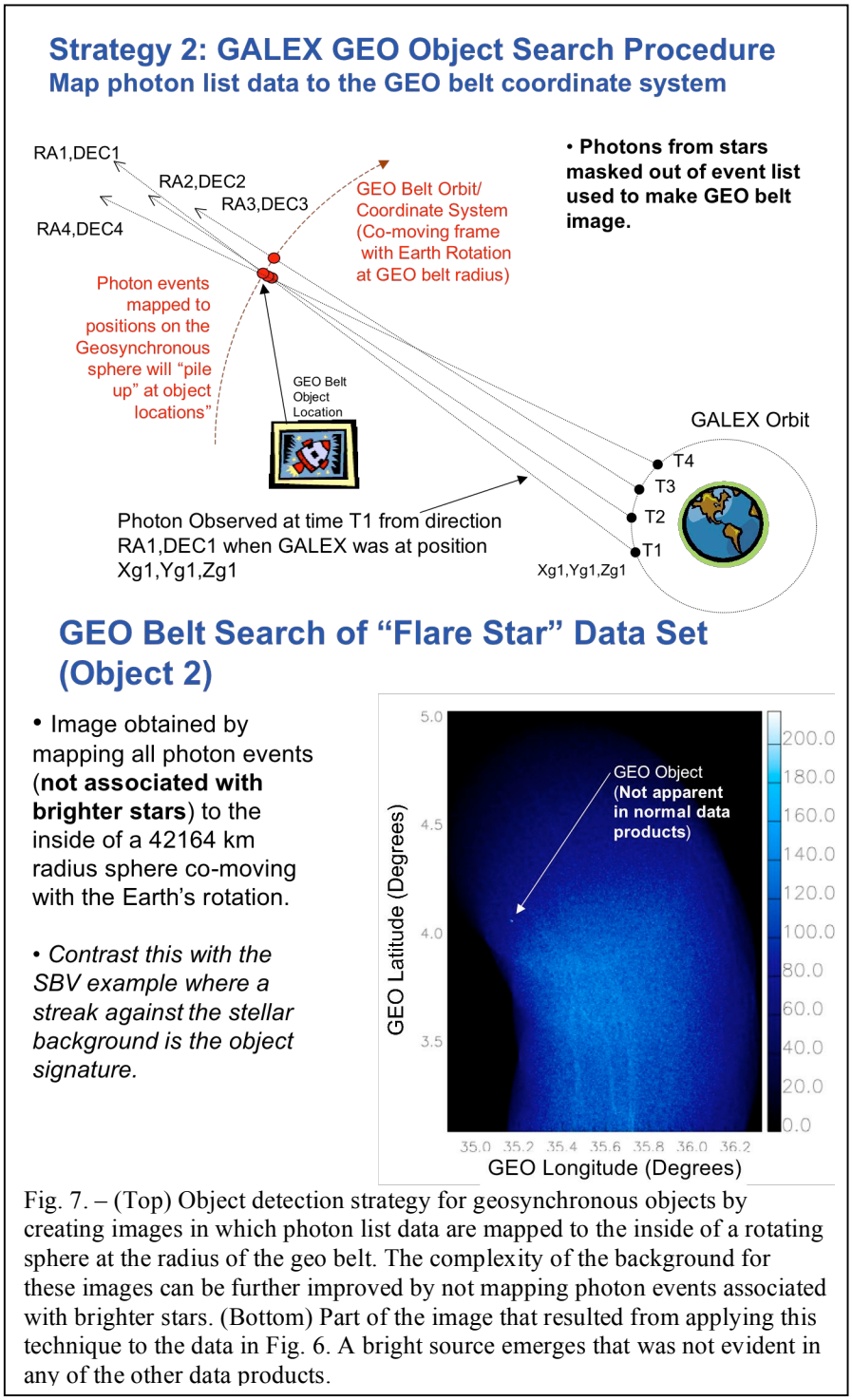

Fig. 7. – (Top) Object detection strategy for geosynchronous objects by creating images in which photon list data are mapped to the inside of a rotating sphere at the radius of the geo belt. The complexity of the background for these images can be further improved by not mapping photon events associated with brighter stars. (Bottom) Part of the image that resulted from applying this technique to the data in Fig. 6. A bright source emerges that was not evident in any of the other data products.

Fig. 6 demonstrates the flexibility in processing and visualizing the GALEX photon list data to examine space objects in the field of view. The image at the upper left is in sidereal coordinates and is the sum of all of the photon events over the 1250 seconds, contrast stretched. There is no obvious evidence in this image that a space object crossed the field of view. In the bottom image, all of the same event data are projected onto a Time-Right Ascension view. The diagonal streak from the object is now quite evident. Fixed stars form purely horizontal streaks in this view. The top middle image corresponds to a sidereal view that is time sliced only around the object passage. Again, the object is clearly visible. The last image at the upper right results from projecting the photon events into a co-moving frame of reference with the object, thereby making the object a "point source". This object will be called "Object #1" in the following metric analysis section of this paper.

Fig. 7 outlines a more sensitive approach using geosynchronous objects as a special case. The photon list data can be mapped to a candidate co-moving coordinate system to look for objects that are moving with those velocities. In the case of geosynchronous belt searches, we create images by mapping the photon events onto the inside of a sphere rotating with the earth at the geosynchronous radius. At the same time, photon events associated with brighter stars can be eliminated from the new projection to help eliminate some of the background clutter. When the same dataset used in Fig. 6 was displayed in this manner, a point source appears that was not evident in any of the sidereal projections. This object will be called "Object 2" in the following analysis section. Object #2 produced only about 2.5 photon events per second (UV magnitude = 19) and was visible for about 160 seconds.

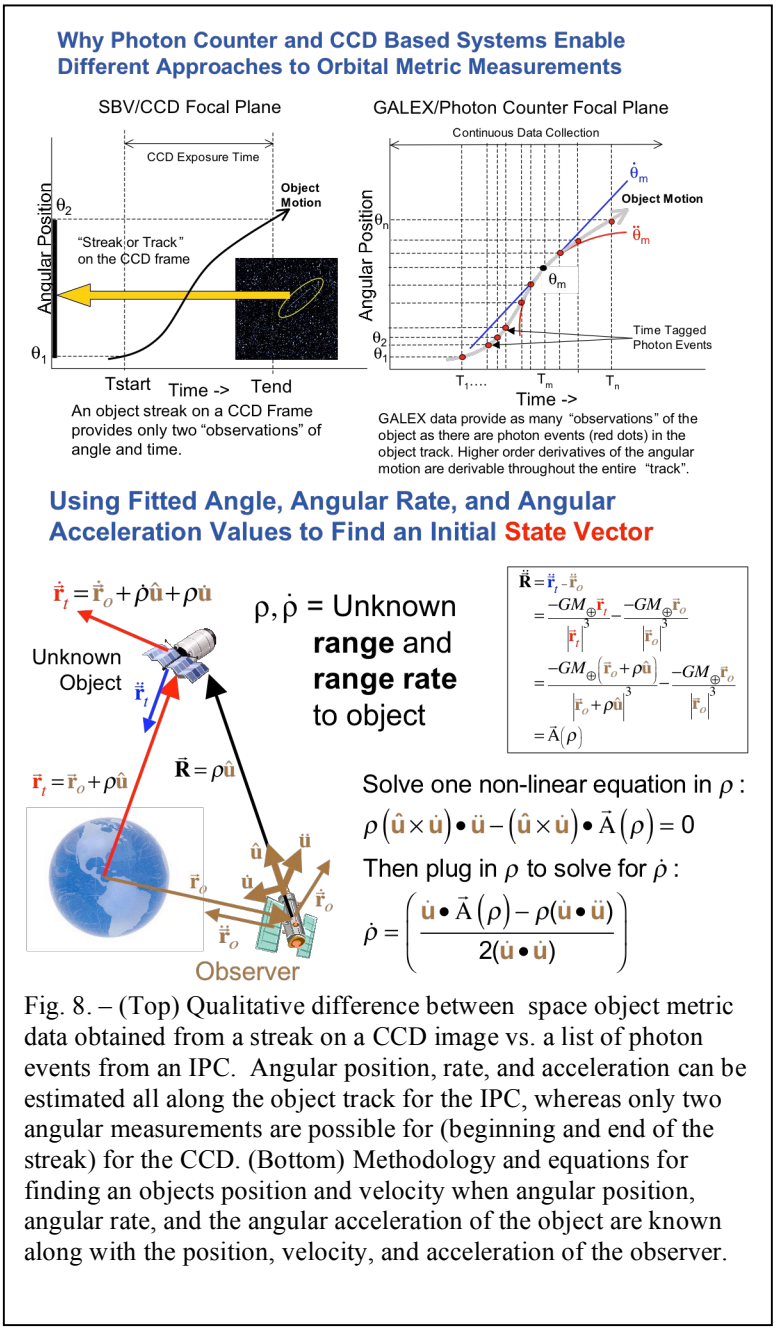

Fig. 8. – (Top) Qualitative difference between space object metric data obtained from a streak on a CCD image vs. a list of photon events from an IPC. Angular position, rate, and acceleration can be estimated all along the object track for the IPC, whereas only two angular measurements are possible for (beginning and end of the streak) for the CCD. (Bottom) Methodology and equations for finding an objects position and velocity when angular position, angular rate, and the angular acceleration of the object are known along with the position, velocity, and acceleration of the observer.

To check if other objects with different types of orbits pass through the GALEX field of view, it is rather straightforward to project the photon list data into a coordinate system that is centered on the location of each suspected object using its orbital elements.

5. METRIC ANALYSIS WITH PHOTON LIST DATA

Once space objects have been identified in a GALEX photon dataset and extracted as a separate list, the events can be analyzed to determine an initial orbit estimate. If the object is known, the time tagged event list can be added to other observations to update an existing ephemeris. We will assume that the two objects detected in the previous section are unknown, and ask how their event lists can be used to generate an initial orbit or state vector estimate. Both Objects #1 and #2 have been identified separately, so we can check on how close our orbital estimates are to the public two line element ephemeris sets. There are several approaches we can use to turn this photon event list into an orbit estimate. The first is to use a Kalman filter (e.g. Orbital Determination Toolkit (ODTK) by Analytical Graphics, Inc [6]). A Kalman filter needs good initial guess for a solution but it can recover sensor biases. A second approach involves orbit determination using three precise angular positions (e.g. method of Gooding [7]). In this approach, we would spline fit in time the photon list Right Ascension and Declination data to determine three high time precision angle sightings and then use in the Gooding approach. However, we want to emphasize the qualitative difference between photon list data and image streak data for orbit determination. Therefore we will show how angular position, rate, and acceleration at a single point in the track derived from a spline fit can be used to determine an initial orbit estimate.

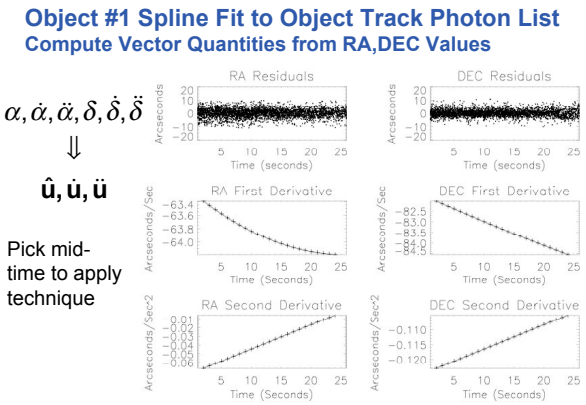

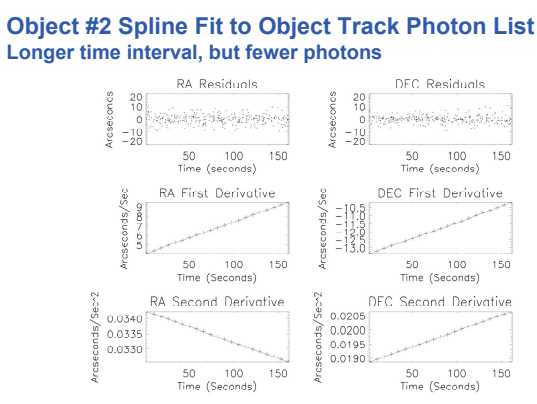

Object #1 == Catalog # 20316: Ariane GTO Upper Stage
Fit Compared to TLE (~4300 Photon Events over 25s)

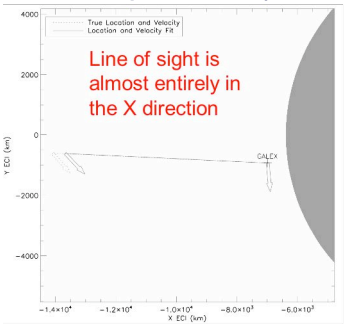

Quantity	Fit	Delta from TLE Value
X ECI (km)	-13761.7	-310.7
Y ECI (km)	-644.2	13.7
Z ECI (km)	-554.0	-5.94
X ECI (km/sec)	4.575	-0.546
Y ECI (km/sec)	-4.650	0.120
Z ECI (km/sec)	0.829	-0.130
	Observed	Delta from TLE Value
RA (Deg.)	177.318	-0.007
DEC (Deg.)	0.243	0.059

Object #2 == Catalog Number 25642: Raduga 1-4
Fit Compared to TLE (~500 Photon Events over 150 s)

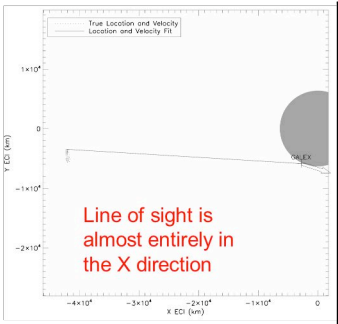

Quantity	Fit	Delta from TLE Value
X ECI (km)	-42139.8	229.6
Y ECI (km)	-3502.6	-18.8
Z ECI (km)	2980.7	-4.6
X ECI (km/sec)	0.211	0.047
Y ECI (km/sec)	-3.0645	0.0009
Z ECI (km/sec)	0.0065	0.0164
	Observed	Delta from TLE Value
RA (Deg.)	176.4910	-0.0069
DEC (Deg.)	0.38615	0.0045

Fig. 10. – (Top Row) Spline fit of RA and DEC photon event data vs. time for objects #1 and #2. The spline fits in RA and DEC are used to compute the angular vector quantities. (Bottom Row) the angular position, rate, and acceleration data from mid-track were used to estimate a state vector and then compared with the published ephemeris for both objects.

In what follows there are some caveats that must be noted. Although GALEX time stamps photons to 5 ms precision, its clock drifts ahead by a few seconds every week. Adjustments are periodically made by the GALEX groundstation to fix this effect, but currently it is difficult to a priori determine this time offset. A time bias was applied to minimize the angular observation offsets due to GALEX's clock bias, but some angular biases between what is predicted from the ephemeredes and the observations remain. Public two line element sets were used for GALEX and the observed objects. Also, public open source ephemeris prediction software was used in the analysis.

Fig. 8 outlines the mathematical procedure. This method uses the fact that GALEX and the unknown space object are both accelerating under the influence of gravity. The acceleration of the unknown object is a known function of the estimated distance from GALEX to the object along the line of sight. We can measure the angular position, the angular rate, and the angular acceleration from a spline fit to the photon list data, which are then used as coefficients of a non-linear equation to solve for the distance to the target. For the spline fit, we used the technique published by Thijsse [9] for robustly estimating the spline in the presence of noise. Once the distance to the target is known, we can also determine the velocity along the line of sight by the second equation in Fig. 8. With these two spatial quantities along with the angular parameters, the full state vector of position and velocity at a fixed time along the objects's track can be determined. However, the non-linear equation for the distance to target can only be solved if the difference between GALEX's and the object's acceleration has a non-zero projection onto the sky as seen by GALEX. In addition, that vector projection of acceleration must be in a direction that has a significant vector component perpendicular to the angular direction of motion as seen by the observer. Another way of saying this is that the acceleration of the target object must be observable when projected onto the sky as seen by the observer. If you are standing under an object accelerating by gravity towards you, you will have no information as to how far away the object is. But if you can observe the falling motion from off to the side and by knowing the value of the acceleration of gravity, then you can estimate it's distance.

Fig. 10 shows the results of spline fits to the angular data for objects #1 and #2 and then subsequently using the mid-track angular values to determine a state vector. The state vectors are also compared with what the predicted values should be using the published two line element sets. Object #1 was identified as a Ariane geosynchronous transfer stage (catalog number 20316) at a range of about 7000 km from GALEX when it passed through its field-of-view. Even though a significant portion of the object's velocity was along the line of sight to GALEX, this method determined the range to target with an accuracy of 5%, and an estimate of the velocity along the line of sight to about 10% using only 25 seconds of passive optical data! If any other information outside of the GALEX observations could have been provided, such as constraints on the orbit inclination, we could have determined a much more accurate estimate of the state vector.

Object #2 was determined to be a geosynchronous object, catalog number 25642. The solution was about 230km off in range but an amazing 47 meters/second off in line of sight velocity, again with only 160 seconds of passive optical data!

6. A NEW IMAGING PHOTON COUNTING IMAGING SYSTEM

DOE/NNSA NA-22 has funded the development of a single photon counting imaging data system that brings photon lists to the USB port on your laptop (See Fig. 11). This system is called NCAM. The first NCAM unit should be fully functional by the end of calendar year 2007. This system would be ideal to couple with ground based optical systems to further explore the space surveillance techniques using photon lists that were outlined in this paper. For further information, contact Dr. Robert Shirey, shirey@lanl.gov, 505-665-5496.

Los Alamos DOE/NNSA Funded Effort: *Ncam*
A Compact & Rugged Single-Photon Imager

Vision

Deliver single-photon imaging & timing capabilities in a tightly integrated camcorder-like form.

NCam mechanical housing – July 2007

Low-Profile

- *Dimensions: ~ 5" x 5" x 12"*
- *Weight: ~ 20 lb*
- *Power: ~ 20-25 W*

Operation Like Digital Camera/Camcorder

- *Instrument operation: Basic On/Off, Standby/Run*
- *Realtime LCD viewfinder option*
- *High-speed data links (USB & TCP/IP) to external computer for higher-level processing & data storage.*
- *Use of COTS lenses (Canon EOS)*
- **POC: Dr. Robert Shirey shirey@lanl.gov**
  505-665-5496 (HERE AT MEETING)

Fig. 11. – LANL NCam system. First unit to be operational by the end of calendar year 2007.

7. CONCLUSIONS

Photon counting imaging sensors enable enhanced object detection capabilities by allowing rate tracking in software after the photon list data are collected. Object track data made up of a time-tagged list of photons can be transformed into precision angle, angular rate, and angular acceleration data that can in turn be used to generate an initial object

state vector. Photon counting imaging sensors allow lower cost concept of operations for sensor platforms because photon counting imagers enable continuous data collection with no smearing or streaking of the stars or space objects, no matter what angular velocities they have. No "point-stabilize-expose-reposition" operations are needed for IPCs. IPCs enable precision surveillance from continuously scanning platforms.

The use of IPCs should be a serious consideration in future design trades for optical space surveillance systems, whether based on the ground or in space.

8. ACKNOWLEDGEMENTS

This work was supported by the Department of Energy National Nuclear Security Agency, Office of Research and Engineering, and carried out at Los Alamos National Laboratory. We acknowledge critical support from the Caltech GALEX Science Team (Chris Martin, PI) and the UC Berkeley Space Sciences Laboratory GALEX detector team (Oswald Siegmund, detector lead). We also wish to thank the support of the LANL Nuclear Nonproliferation and Department of Defense Program Offices. Joe Bergin, Paul Schumacher, Laura Ulibarri, Barry Hogge at AFRL/DE and Matt Fettrow and Tom Caudill of AFRL/VS provided many useful insights and comments. LANL staff members James Theiler and Heath Davis provided invaluable help with statistical issues and the orbit determination method of Gooding respectively.

9. REFERENCES

1. Oswald Siegmund, Barry Welsh, John Vallerga, Anton Tremsin, and Jason McPhate, "High performance microchannel plate imaging photon counters for spaceborne sensing", *Proc. SPIE Vol. 6220*, 622004 (May. 30, 2006)

2. M. H. Baron and W. C. Priedhorsky, "Crossed Delay Line Detector for Ground and Space Based Applications", *EUV, X-Ray, and Gamma-Ray Instrumentation for Astronomy IV*, Oswald H. Siegmund,ed., Proc. SPIE 2006, 188-197 (1993).

3. Martin, D C; Fanson, J.; Schiminovich, D.; Morrissey, P.; Friedman, PG; Barlow, TA; Conrow, T.; Grange, R.; Jelinsky, PN; Milliard, B.; et. al. "The Galaxy Evolution Explorer: a space ultraviolet survey mission", *Astrophysical Journal Letters,* 20 Jan. 2005; vol.619, no.1, pt.1, p.L1-6.

4. Priedhorsky, W, Bloch, J J, "Optical detection of rapidly moving objects in space", *Applied Optics*, 20 Jan. 2005, vol.44, no.3, p.423-33.

5. Stokes, G H., Von Braun, C., Sridharan, R., Harrison, D., Sharma, J., "The Space-Based Visible Program", *Lincoln Laboratory Journal*, Volume 11, Number 2, Page 205, 1998.

6. Orbit Determination Toolkit by Analytical Graphics, Inc., http://www.agi.com/products/desktopApp/odtk/

7. Gooding, R H., "A new procedure for the solution of the classical problem of minimal orbit determination from three lines of sight", *Celestial Mechanics and Dynamical Astronomy*, 1996-1997; vol.66, no.4, p.387-423

8. Thijsse, B J, Hollanders, M A, Hendrikse, J, "A practical algorithm for least-squares spline approximation of data containing noise.", *Computers in Physics*, July-Aug. 1998, vol.12, no.4, p.393-9.